AN EFFICIENCY OPTIMIZATION OF A POLYSILICON PHOTOVOLTAIC MODULE USING A 2-D ANALYTICAL AND A TWO-DIODE I-V MODEL FOR AN ILLUMINATED SOLAR CELL

Sami Kolsi, Hekmet Samet[1] and Mohamed Ben Amar[2]
ACEM Research Unit, Department of Electrical Engineering, National Engineering School of Sfax, BP.W 3038, Sfax, Tunisia
[1] Electronic Laboratory and Information Technology, Department of Electrical Engineering, National School Engineering of Sfax, BP.W 3038 ,Sfax, Tunisia
[2] Department of Physics, Science Faculty of Sfax, BP. 802, 3038, Sfax, Tunisia
sami_kolsi@yahoo.fr

(Received 30 June 2009 - Accepted 14 May 2010)

ABSTRACT

A two-dimensional (2D) analytical model based on the Green's Function method is applied on a n^+-p polysilicon solar cell. This model is implemented through a simulation program in order to optimize the conversion efficiency of a PV module constituted of 36 solar cells connected in series. The influence of different physical and geometric parameters like doping density and thickness of different regions of the elementary cell on the conversion efficiency. This study shows that the optimum conversion efficiency of the considered PV module can reach 19,38 %. A half-analytical method was investigated while using a two-diode I-V model to predict the five electrical parameters that characterize the I-V relationship of PV module. These results are in satisfactory agreement with the simulation model of other works.

Keywords: polysilicon, conversion efficiency, optimization, photovoltaic module

Nomenclature
I_{ph} : PV module generated current (A).
I_{d0}: PV module saturation diffusion dark current (A).
I_{r0} : PV module saturation recombination (A).
R_s: PV module series resistance (Ω).
R_{sh} : PV module shunt resistance (Ω).
I: output current (A).
V: voltage delivered by PV module (V).
I_m : current at maximum power point (A).
V_m : voltage at maximum power point (V).
S: single effective cell area (m^2).
q : electron charge ($1,6\ 10^{-19}$ C).
T_c: cell temperature (K).

P_i : incidence irradiance under AM1 illumination condition on the PV cell surface.
I_{sc} : short circuit current (A).
V_{oc}: open circuit voltage (V).
FF: fill factor.
η: conversion efficiency of PV module.
V_T: thermal voltage (V).
W_e: emitter thickness (µm).
W: space charge region width (µm).
W_b: base layer thickness (µm).
S_n: PV cell recombination velocity at the rear contact (cm/s).
S_p: PV cell recombination velocity at the front contact (cm/s).
V: limit perpendicular recombination velocity of the emitter (cm/s).
$V_{g,i}$: grain boundary recombination velocity related to the incident wavelength λ_i (cm/s).
H: thickness of semiconductor (µm).
d : grain size (µm).
D : cell dimension (µm).
N_A : doping density of base (cm^{-3}).
N_D : doping density of emitter(cm^{-3}).
N_s: number of cells in series=36.
K: Boltzmann's constant.
n_i : silicon intrinsic carrier concentration.
ε_o : emptiness permittivity.
ε_r : relative silicon permittivity.
α_i : absorption coefficient related to the incident wavelength λ_i (μm^{-1}).
g_i : silicon generation rate related to the incident wavelength λ_i ($cm^{-3}s^{-1}$).
D_n: diffusion constant of electrons (cm^2/s).
D_p: diffusion constant of holes (cm^2/s).
L_n: diffusion length of electrons (cm).
L_p: diffusion length of holes (cm).
τ_n: electrons lifetime (s).
τ_p: holes lifetime (s).
μ_n: mobility of electrons ($cm^2.V/s$).
μ_p: mobility of holes ($cm^2.V/s$).

INTRODUCTION

The most important factor that characterizes the performance of solar cells is the conversion efficiency. Increasing efforts made for improving the conversion efficiency while reducing the manufacturing cost of solar cells have required the study of the influence of several parameters on the performance of solar cells. This study requires a structure modelling of the considered cell. Several authors have presented different structure to model a cell (Ben Arab, 1997; Dugas, 1996; Ba & Kane, 1995; Belghachi & Helmaoui, 2008; Kotsovos & Perraki, 2005; Liou & Wong, 1992; Dugas, 1994; Zhao *et al.*, 2009; Diallo *et al.*, 2008).

The aim of this work is the optimization of efficiency conversion of polysilicon PV module taking into account some physical and geometric parameters of an elementary cell such as doping density carriers and thickness of different regions of the cell. The photogenerated and dark current of a polycrystalline solar cell have been determined while

using a 2-D analytical model based on Green method (Dugas & Oualid, 1987; Green, 1978; Halder & Williams, 1983).

A two-diode electrical model was also used which allows us to determine the current-voltage characteristic and efficiency of PV module that constituted of 36 elementary solar cells connected in series. Based on this model, a half-analytical method was investigated in order to find the five electrical parameters that characterize the I-V relationship of PV module. It is assumed that cells have the same physical and geometric properties and present the same illuminated current-voltage characteristics. Finally, investigation of this model shows a reliable performance since these results are in satisfactory agreement with the available simulated I-V characteristic results obtained by the work of Van Dyk and Meyer (2004) using PVSIM software (King *et al*., 1996).

MATERIALS AND METHODS

Model of the elementary solar cell

The structure of the poly Si solar cell (Figure1) is divided into three main regions (emitter (n^+), space charge region (n^+-p) and base region (p)). According to this model, the thickness of each region is W_e, W and W_b respectively.

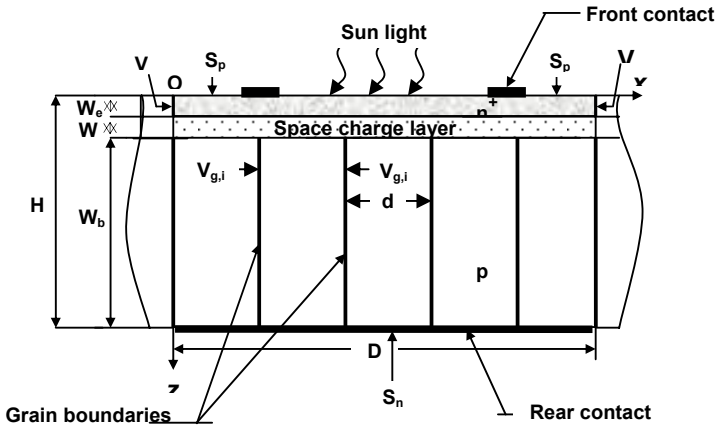

Figure 1. A two dimensional physical model of a cell used in simulation).

The following considerations have been introduced in order to simplify this model:
(i) The poly Si grains are assumed as columnar and perpendicular to the n^+-p junction (Dugas & Oualid, 1987), and their electrical properties are homogeneous (doping concentration, minority carrier mobility, lifetime and diffusion length).
(ii) The minority carrier mobility and lifetime in both base and emitter region depends only on the doping level for the corresponding region.
(iii) Uniform doping profiles for each for the three quasi-neutral regions are assumed.

(iv) Grain boundary recombination is negligible in the heavily doped emitter (Dugas & Oualid, 1987) and in the junction space charge region (Dugas *et al.*, 1983). This is in agreement with Green (1978).
(iv) It is assumed that low-level injection conditions prevail.

Electrical model of PV module

In this study, the PV model composed of 36 elementary solar cells connected in series is considered. The I-V characteristic of the PV module can be obtained if one considers the equivalent circuit model represented in (Figure 2).

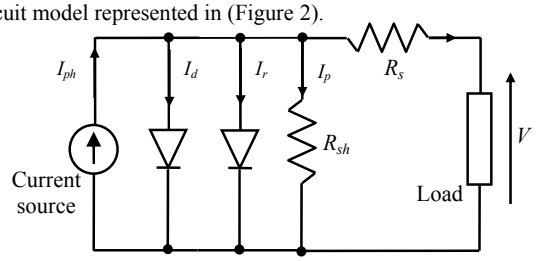

Figure 2. Two-diode equivalent circuit for PV module.

In this model, the recombination at the surface and in the bulk is considered which is expressed by R_s and by R_{sh} respectively. So, using Kirchhoff's first law, the current I is given by:

$$I = I_{ph} - I_d - I_r - I_p \tag{1}$$

Using Eq. (1), we propose the following two-diode I-V characteristic relating to the considered module:

$$I = N_p I_{ph} - N_p I_{d0}\left[\exp\left(\frac{\frac{V}{N_s}+R_s\frac{I}{N_p}}{V_T}\right)-1\right] - N_p I_{r0}\left[\exp\left(\frac{\frac{V}{N_s}+R_s\frac{I}{N_p}}{2V_T}\right)-1\right] - \frac{\frac{V}{N_s}+R_s\frac{I}{N_p}}{R_{sh}} \tag{2}$$

Where $V_T = \dfrac{KT_c}{q}$

N_p=1 in the considered PV module.

The fill factor of module is given by:

$$FF = \frac{I_m V_m}{I_{sc} V_{oc}} \tag{3}$$

The conversion efficiency of the module is given by:

$$\eta = \frac{I_m V_m}{S N_s P_i} \tag{4}$$

The photogenerated current I_{ph} delivered by the low efficiency cell, the saturation diffusion dark current I_{d0} and the saturation recombination current I_{r0} are given by Eqs. (A.8), (A.14), (A.15),(A.24),(A.25) and (A.28) in Appendix.

V_m is the sum of the maximum voltage delivered by the associated cells, I_{sc} represents the short-circuit current of the connected cells and V_{oc} is the sum of the open-circuit voltage of each cell.

In order to calculate $I_{ph,}$, I_{d0}, I_{r0}, R_s and R_{sh}, the half analytical method is used to solve the equation system below (5) to (9) knowing the values of I_m, V_m, I_{sc} and V_{oc} given as:

(i) For short circuit current: $\mathrm{I} = \mathrm{I}_{sc}, \mathrm{V} = 0$

$$I_{sc} = I_{ph} - I_{d0}\left[\exp\left(\frac{R_s I_{sc}}{V_T}\right) - 1\right] - I_{r0}\left[\exp\left(\frac{R_s I_{sc}}{2V_T}\right) - 1\right] - \frac{R_s I_{sc}}{R_{sh}} \tag{5}$$

(ii) For open circuit voltage: $\mathrm{I} = 0, \mathrm{V} = \mathrm{V}_{oc,mod}$

$$I_{ph} - I_{d0}\left[\exp\left(\frac{V_{oc}}{N_s V_T}\right) - 1\right] - I_{r0}\left[\exp\left(\frac{V_{oc}}{2N_s V_T}\right) - 1\right] - \frac{V_{oc}}{N_s R_{sh}} = 0 \tag{6}$$

(iii) At maximum power point: $\mathrm{I} = \mathrm{I}_m, \mathrm{V} = \mathrm{V}_m$

$$I_m = I_{ph} - I_{d0}\left[\exp\left(\frac{\frac{V_m}{N_s} + R_s I_m}{V_T}\right) - 1\right] - I_{r0}\left[\exp\left(\frac{\frac{V_m}{N_s} + R_s I_m}{2V_T}\right) - 1\right] - \frac{\frac{V_m}{N_s} + R_s I_m}{R_{sh}} \tag{7}$$

(iv) $$I_x = I_{ph} - I_{d0}\left[\exp\left(\frac{\frac{V_x}{N_s} + R_s I_x}{V_T}\right) - 1\right] - I_{r0}\left[\exp\left(\frac{\frac{V_x}{N_s} + R_s I_x}{2V_T}\right) - 1\right] - \frac{\frac{V_x}{N_s} + R_s I_x}{R_{sh}} \tag{8}$$

(v) $$I_{xx} = I_{ph} - I_{d0}\left[\exp\left(\frac{\frac{V_{xx}}{N_s} + R_s I_{xx}}{V_T}\right) - 1\right] - I_{r0}\left[\exp\left(\frac{\frac{V_{xx}}{N_s} + R_s I_{xx}}{2V_T}\right) - 1\right] - \frac{\frac{V_{xx}}{N_s} + R_s I_{xx}}{R_{sh}} \tag{9}$$

Where $V_x = \frac{V_m}{2}$ and $I_{xx} = \frac{I_m}{2}$

RESULTS AND DISCUSSION

Validation of this approach

In order to validate this model by using the half-analytical method based on the two-diode model, the results obtained from this approach are compared by using MAPLE software to the simulation results obtained from the study developed by Van Dyk and Meyer (2004) and established by PVSIM software (King *et al*., 1996). The PVSIM software uses in its library the two-diode model of an elementary solar cell.

Based on the required five data points of interest on the given simulation current-voltage characteristic (Figure 3), the five parameters (I_{ph}, I_{d0}, I_{r0} R_s and R_{sh}) are extracted using a system of Eqs (5) to (9). Then based on Eq (2), the corresponding I-V characteristic is presented. Then, V_{oc}, I_{sc} and P_m are calculated while using Eqs (5) to (7). (Figure 3) shows the I-V characteristic for the polycrystalline PV module gotten from the PVSIM software simulation and from this approach. A satisfactory agreement between this approach and the simulation results is found.

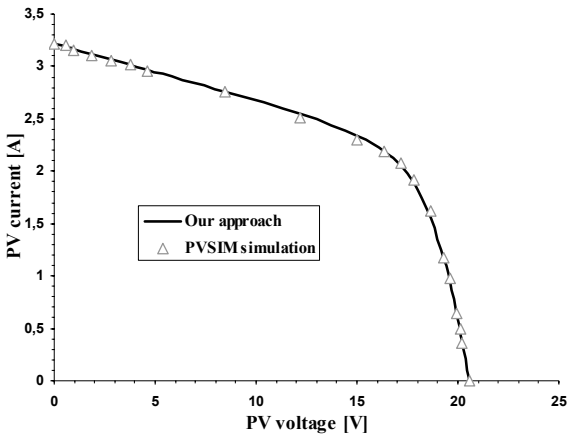

Figure 3. I-V characteristic for PV module gotten from PVSIM simulation and from this approach.

Table 1 illustrates the photovoltaic parameters of the considered PV module obtained by PVSIM simulation and by computation from this model and gives accuracy in each parameter. The photovoltaic parameter values obtained from this model are very close to the simulation results.

It is noticed that, this method is very efficient compared with PVSIM simulation because it allows to determine the photogenerated current, the saturation diffusion dark current I_{d0} and the saturation recombination current I_{r0} of the module expressed as a function of technological parameter of solar cell. So, using these parameters, one can optimize the conversion efficiency of PV module.

TABLE 1

Comparison between the Photovoltaic Parameters of the Module Gotten from This Model and Those by PVSIM Simulation

Parameters	R_{sh} (Ω)	R_s (Ω)	I_{sc} (A)	I_{d0}(nA)	I_{r0} (μA)	I_{ph} (A)	V_{oc} (V)	P_m (W)	FF (%)
PVSIM simulation[1]	18	0,36	3,22	-	-	-	20,64	35,85	54
Our model	18,036	0,3614	3,2194	0,2945	10,35	3,284	20,64	35,847	53,945
Error (%)	0,2	0,38	0,018	-	-	-	0	0,008	0,1

[1] The simulations were done using 1000 W/m^2 irradiance and 25°C cell temperature.

Optimization of module conversion efficiency

In order to optimize the performances of PV module, the conversion efficiency behaviour was analyzed with respect to physical and geometric parameters. The results developed in this section are established with the following parameters values listed in (Table 2).

Is is noticed that this study is made in the case of an advanced treatment of grain boundaries of an elementary cell constituting the module. The value of the recombination velocity of such boundaries which depends on the incident wavelength is illustrated in (Table A.1) in appendix.

Figure 4 shows the variation of the conversion efficiency module with respect to the recombination velocity S_p at the front contact of cells. Efficiency conversion decreases when S_p increases. A maximum of conversion efficiency can be obtained for a surface treatment allowing the recombination velocity to decrease until 3×10^2 cm/s.

TABLE 2

Physical Parameters of an Elementary Cell Used in the Computation Results

Parameters	Value
T_c (K)	300
ε_r	11,8
n_i (cm^{-3})	$1{,}45\times10^{10}$
$R_{sh,mod}$ (Ω)	360
V (cm/s)	10^3
K (J/K)	$1{,}3806\times10^{-23}$
ε_o (F.cm^{-1})	$8{,}85\times10^{-14}$
$R_{s,mod}$ (Ω)	0,126
S (m^2)	10^{-2}
P_i (W/m^2)	925

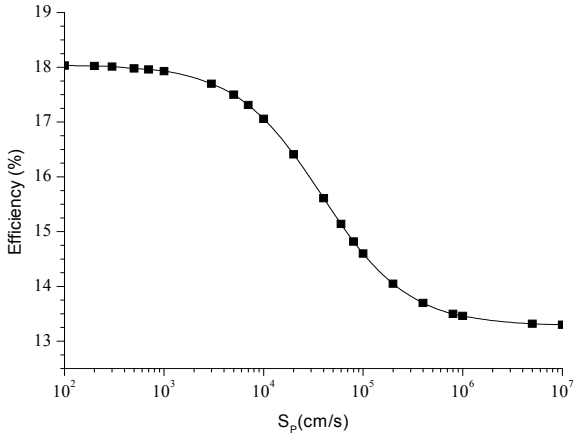

Figure 4. Conversion efficiency of PV module versus velocity recombination in front contact S_p (S_n=10^4cm/s, N_A=10^{16}cm^{-3}, N_D=10^{19}cm^{-3}, d=60µm, W_b=300µm, W_e=1µm).

Figure 5 shows the effect of emitter thickness W_e on conversion efficiency. When W_e<1µm, efficiency is constant, then, it decreases sharply when W_e increases. Indeed, the generation of carriers in base region decreases in favour of the one in the emitter. However, the supplementary carriers generated in the emitter are not collected to the limit of space charge layer when the diffusion length L_p becomes less than W_e.

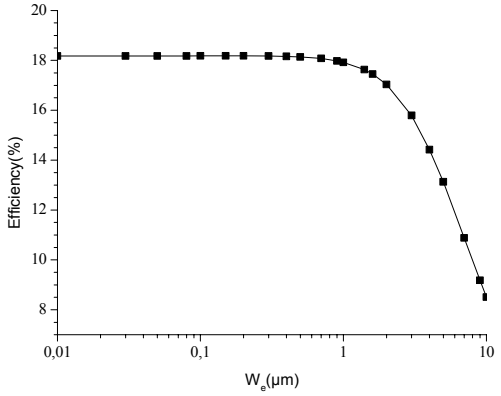

Figure 5. Conversion efficiency of PV module versus emitter thickness W_e (S_n=10^4cm/s, N_A=10^{16}cm^{-3}, N_D=10^{19}cm^{-3}, d=60µm, W_b=300µm, S_p=10^3cm/s).

Figure 6 stands for the variation of the conversion efficiency module as function of base thickness W_b. For $10\mu m<W_b<200\mu m$, one notes that efficiency increases considerably with W_b, then becomes practically constant for $W_b>300\mu m$. In fact, the minority carriers diffusion length L_n in the base region is equal to 306µm. So, the optimal thickness of base $W_{b,opt}$ is on the order of the minority carriers diffusion length. This result is in agreement with the one found by Kotsovos and Perraki (2005).

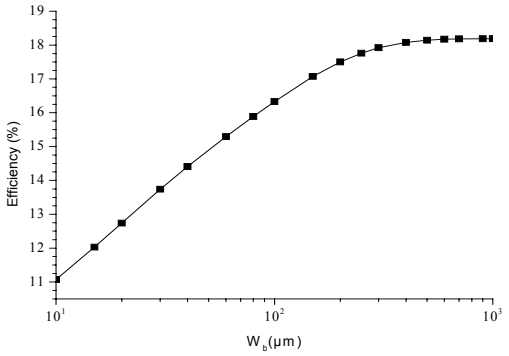

Figure 6. Conversion efficiency of PV module versus base thickness W_b ($S_n=10^4$cm/s, $N_A=10^{16}$cm^{-3}, $N_D=10^{19}$cm^{-3}, d=60µm, W_e=1µm, $S_p=10^3$cm/s).

Figure 7 demonstrates the influence of grain size d on conversion efficiency. One remarks that efficiency increases versus d (Dugas, 1994). For d<300µm, efficiency depends a great deal on grain size. For d>300µm, the efficiency variation with d becomes weaker. Indeed, for an advanced treatment, the recombination at grain boundaries is important when the grain width becomes weak (Kotsovos & Perraki, 2005).

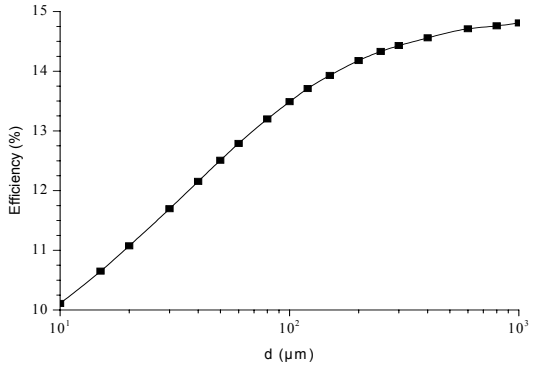

Figure 7. Conversion efficiency of PV module versus grain sizes d ($S_n=10^4$cm/s, $N_A=10^{16}$cm^{-3}, $N_D=10^{19}$cm^{-3}, W_b=300µm, W_e=1µm, $S_p=10^3$cm/s).

Figure 8 shows the variation of conversion efficiency of a module as function of doping density level of base region N_A. One can see that efficiency increases with N_A to reach a maximum value for $N_{A,opt}=2\times10^{16}cm^{-3}$. This result is comparable to the one established by Dugas (Dugas & Oualid, 1987). For $N_A>N_{A,opt}$, the efficiency falls abruptly, and this is due to the recombination of photogenerated carriers in the base bulk when the diffusion length L_n becomes less than W_b.

Figure 9 presents the variation of the efficiency module according to the emitter doping density N_D. For $N_D<10^{19}$ cm^{-3}, one can notice that the efficiency is practically constant and it reaches its maximum for $N_{D,opt}=2\times10^{18}cm^{-3}$. When $N_D>10^{19}$ cm^{-3}, the efficiency decreases rapidly. In fact, the bulk recombination in the emitter region increases with N_D and the photocurrent in space charge layer decrease.

Figure 10 shows the effect of the recombination velocity S_n at rear contact on conversion efficiency. It can be seen that the efficiency depends weakly on S_n. Indeed, the relative variation on efficiency versus S_n is approximately 2,56%. This result justifies the ohmic rear contact in the industrial manufacturing of solar cells when the base thickness considered is practically equal to the diffusion length L_n

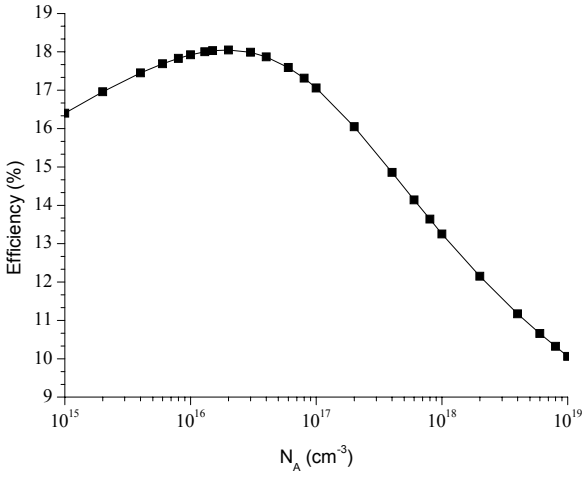

Figure 8. Conversion efficiency of PV module versus doping concentration level of base N_A ($S_n=10^4$cm/s, d=60µm, $N_D=10^{19}cm^{-3}$, W_b=300µm, W_e=1µm, $S_p=10^3$cm/s).

From the previous study, Table 3 presents the optimal values of different physical and geometrical parameters of the module.

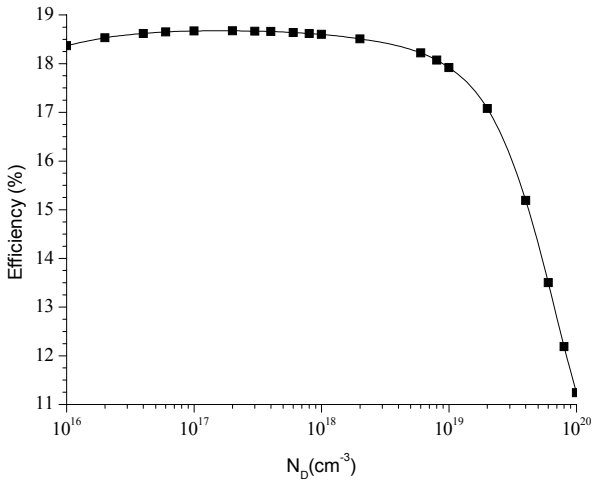

Figure 9. Conversion efficiency of PV module versus doping concentration level of emitter N_D ($S_n=10^4$cm/s, d=60µm, $N_A=10^{16}cm^{-3}$, W_b=300µm, W_e=1µm, $S_p=10^3$cm/s).

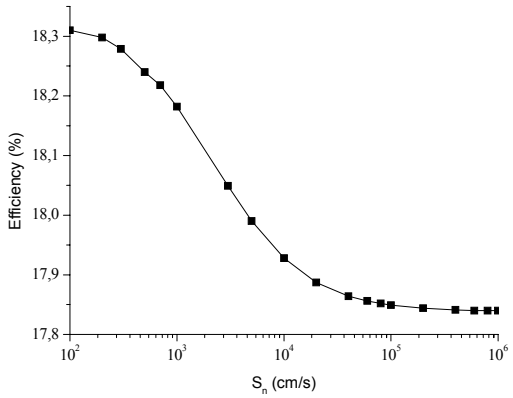

Figure 10. Conversion efficiency of PV module versus recombination velocity at rear contact S_n ($N_A=10^{16}cm^{-3}$, d=60µm, $N_D=10^{19}$cm-3, W_b=300µm, W_e=1µm, $S_p=10^3$cm/s).

TABLE 3

Optimal Values of Different Physical and Geometric Parameters of Module

N_A (cm^{-3})	N_D (cm^{-3})	W_e (µm)	W_b (µm)	S_n (cm/s)	S_p (cm/s)
2×10^{16}	2×10^{18}	1	L_n	10^6	3×10^2

Using the optimal values of the technological parameters of the multicrystalline elementary solar cell, we can determine the photovoltaic parameters of the module. These parameters are illustrated in (Table 4).

TABLE 4

Optimal Parameters of PV Module

$I_{sc,mod}$ (A)	$V_{oc,mod}$(V)	$I_{m,mod}$ (A)	$V_{m,mod}$(V)	P_m (W)	FF_{mod} (%)	η_{mod} (%)
3,93	21,32	3,61	17,85	64,56	76,97	19,38

Based on this table, it is noted that the optimal efficiency of the polysilicon PV module can reach 19,38%.

CONCLUSION

In this paper, a new approach was presented using a two-diode I-V characteristic model whish allows to determine the different photovoltaic parameters of polysilicon photovoltaic module made by connections of elementary cells in series. A remarkable agreement is found when one compares computed results using this model with the available results simulated by PVSIM software.

A 2-D dimensional physical model is also applied for the simulation of the elementary n^+-p poly Si solar cell. The study of the influence of grain size, the recombination velocity at the front and back contact of cells, thickness of base and emitter layer, base and emitter doping density on solar cell efficiency under AM1 irradiance condition is investigated.

This study has shown that the maximum efficiency can be obtained for a n^+-p elementary cell characterized by the emitter thickness to 1µm and doping density to 2×10^{18} cm^{-3} and base thickness in the order of the diffusion length of carriers in base region and doping level to 2×10^{16} cm^{-3}. The dimension of the grains affects the conversion efficiency for high recombination velocities at the grain boundaries and for a base thickness lower than a diffusion length of minority carriers in p region.

Finally, with these optimal physical and geometric parameters, it is shown that conversion efficiency of the considered PV module can reach 19,38%.

APPENDIX

Photogenerated current

The minority carrier density Δn generated in base region can be obtained by solving the two-dimensional continuity equation for electron which is given by:

$$\frac{\partial^2 \Delta n}{\partial z^2} + \frac{\partial^2 \Delta n}{\partial x^2} - \frac{\Delta n}{L_n^2} = -\frac{g_i(z)}{D_n} \tag{A.1}$$

Where:

$$g_i(z) = g_{i,0} \exp(-\alpha_i z)$$

L_n is the minority carrier diffusion length, D_n is the corresponding diffusion coefficient, α_i is the absorption coefficient related to the incident wavelength λ_i and $g_{i,0}$ is the silicon generation rate related to the incident wavelength λ_i.

The boundary conditions for the base region are:

$$\Delta n_i(x, z = W_e + W) = 0 \tag{A.2}$$

$$\left.\frac{\partial \Delta n_i}{\partial z}\right|_{z=H} = \frac{-S_n}{D_n} \Delta n_i(x, z = H) \tag{A.3}$$

$$\left.\frac{\partial \Delta n_i}{\partial x}\right|_{x=0} = \frac{V_{g,i}}{2D_n} \Delta n_i(x = 0, z) \tag{A.4}$$

$$\left.\frac{\partial \Delta n_i}{\partial x}\right|_{x=d} = \frac{-V_{g,i}}{2D_n} \Delta n_i(x = d, z) \tag{A.5}$$

Where S_n is the recombination velocity at the rear contact, d is the grain size and $V_{g,i}$ is the effective recombination velocity at the grain boundary related to incident wavelength λ_i. $V_{g,i}$ can be obtained by the physical model of grain boundary recombination in polysilicon (Oualid *et al*., 1984; Joshi P & Bhatt, 1990; Ben Amar & Ben Arab, 2001). In this study, the model developed by Ben Amar and Ben Arab (2001) is considered. It demonstrates the dependence of V_g on the incident wavelengths.

In order to calculate the total minority carrier density generated in the base region using AM1 illumination condition, the assumption proposed by Mohammed and Rogers (1988) which decomposes the solar spectrum in four wavelengths is considered. Absorption coefficient and generation rate in AM1 illumination condition α_i (μm^{-1}) and $g_{i,0}$ ($cm^{-3}s^{-1}$) and grain boundary recombination velocity $V_{g,i}$ related to the incident wavelength λ_i, are given in (Table A.1) (Ben Amar & Ben Arab, 2003; Mohammed *et al*., 1989).

TABLE A.1

Absorption Coefficientα_i, Generation Rate g_i and Grain Boundary Recombination Velocity $V_{g,i}$ Related to the Incident Wavelength λ_i

Wavelength λ_i	λ_1	λ_2	λ_3	λ_4
α_i (μm^{-1})	$6{,}33079\times10^{-2}$	$1{,}02664\times10^{-2}$	$1{,}47109\times10^{-3}$	1,76058
g_i ($cm^{-3}s^{-1}$)	$6{,}46746\times10^{19}$	$5{,}54674\times10^{18}$	$9{,}26415\times10^{17}$	$2{,}03553\times10^{21}$
$V_{g,i}$ with advanced treatment (cm/s)	5×10^2	6×10^2	$6{,}5\times10^2$	10^2

The total photocurrent I_{ph} relating to the considered cell is given by:

$$I_{ph} = I_B + I_E + I_R \qquad \text{where:}$$

I_B and I_E stand photocurrent in base and emitter region given by the following formula:

$$I_B = S' J_b = \frac{S' q D_n}{d} \int_0^d \frac{\partial \Delta n(x,z)}{\partial z}\Big|_{z=We+W} dx \tag{A.6}$$

$$I_E = S' J_e = \frac{S' q D_p}{D} \int_0^D \frac{\partial \Delta p(x,z)}{\partial z}\Big|_{z=We} dx \tag{A.7}$$

I_R is the photocurrent in space charge layer given as follows (Sze, 1991):

$$I_R = S' \sum_{i=1}^{4} \frac{q g_i \exp(-\alpha_i W_e)}{\alpha_i} \left[1 - \exp(-\alpha_i W)\right] \tag{A.8}$$

Where $S' = 10^4 S$ is the effective area of an elementary cell.

W is the space charge layer of the n^+-p junction; its value is determined using the fully depleted layer model of a n^+-p junction (Sze, 1991), then:

$$W = \left[\frac{2\varepsilon_0 \varepsilon_r}{q^2 N_A} KT Log\left(\frac{N_A N_D}{n_i^2} \right) \right]^{0.5} \tag{A.9}$$

While using Green function method (Dugas, 1994; Dugas & Oualid, 1987; Hovel, 1975), and while accounting to the previously boundary condition, the excess minority carrier density of electron Δn in base region can be given by the general formula:

$$\Delta n(x,z) = \sum_{i=1}^{4} \sum_{k=1}^{\infty} f_{k,i}(z) \cos\left(C_{k,i}(x - d/2)\right) \tag{A.10}$$

The $C_{k,i}$ coefficients are solution of the following transcendent equation (Dugas, 1994):

$$tg\left(C_{k,i}\frac{d}{2}\right)=\frac{V_{g,i}}{2D_nC_{k,i}} \tag{A.11}$$

The general solution of $f_{k,i}$ is expressed under the shape:

$$f_{k,i}(z)=\frac{4g_i\sin\left(C_{k,i}\frac{d}{2}\right)L_{k,i}{}^2}{D_n\left(C_{k,i}d+\sin\left(C_{k,i}d\right)\right)\left(1-\alpha_i{}^2L_{k,i}{}^2\right)}\times \tag{A.12}$$
$$\left\{\frac{\left(\frac{D_n\alpha_i}{S_n}-1\right)\exp(-\alpha_iH)sh\left(\frac{z-\left(W_e+W\right)}{L_{k,i}}\right)-\exp\left[-\alpha_i\left(W_e+W\right)\right]\left[sh\left(\frac{H-z}{L_{k,i}}\right)+\frac{D_n}{L_{k,i}S_n}ch\left(\frac{H-z}{L_{k,i}}\right)\right]}{sh\left(\frac{W_b}{L_{k,i}}\right)+\frac{D_n}{L_{k,i}S_n}ch\left(\frac{W_b}{L_{k,i}}\right)}+\exp(-\alpha_iz)\right\}$$

Where :

$$\frac{1}{L_{k,i}{}^2}=C_{k,i}{}^2+\frac{1}{L_n{}^2} \tag{A.13}$$

Using the formula given by equation (A.6), the current in base region can be rewritten as:

$$I_B=S'\sum_{k=1}^{\infty}\sum_{i=1}^{4}\frac{8qg_i\sin\left(C_{k,i}\frac{d}{2}\right)^2L_{k,i}}{dC_{k,i}\left(C_{k,i}d+\sin\left(C_{k,i}d\right)\right)\left(1-\alpha_i{}^2L_{k,i}{}^2\right)}\times \tag{A.14}$$
$$\left\{\frac{\left(\frac{D_n\alpha_i}{S_n}-1\right)\exp\left(-\alpha_iH\right)+\exp\left[-\alpha_i\left(W_e+W\right)\right]\left[ch\left(\frac{W_b}{L_{k,i}}\right)+\frac{D_n}{L_{k,i}S_n}sh\left(\frac{W_b}{L_{k,i}}\right)\right]}{sh\left(\frac{W_b}{L_{k,i}}\right)+\frac{D_n}{L_{k,i}S_n}ch\left(\frac{W_b}{L_{k,i}}\right)}-L_{k,i}\alpha_i\exp\left[-\alpha_i\left(W_e+W\right)\right]\right\}$$

Using the same method, the emitter current I_E is expressed by:

$$I_E=S'\sum_{j=1}^{\infty}\sum_{i=1}^{4}\frac{-8qg_i\sin\left(C_j\frac{D}{2}\right)^2L_j}{DC_j\left(C_jD+\sin\left(C_jD\right)\right)\left(\alpha_i{}^2L_j{}^2-1\right)}\times\left\{\frac{\left(\frac{D_p\alpha_i}{S_p}+1\right)-\exp\left(-\alpha_iW_e\right)\left(ch\left(\frac{W_e}{L_j}\right)+\frac{D_p}{L_jS_p}sh\left(\frac{W_e}{L_j}\right)\right)}{sh\left(\frac{W_e}{L_j}\right)+\frac{D_p}{L_jS_p}ch\left(\frac{W_e}{L_j}\right)}-L_j\alpha_i\exp\left(-\alpha_iW_e\right)\right\} \tag{A.15}$$

The C_j coefficients are solution of the following transcendent equation (Dugas, 1994):

$$tg\left(C_j\frac{D}{2}\right)=\frac{V}{2D_pC_j} \tag{A.16}$$

Where:

$$\frac{1}{L_j{}^2}=C_j{}^2+\frac{1}{L_p{}^2} \tag{A.17}$$

μ_n and τ_n are respectively the electrons mobility and lifetime given by (Masetti *et col*., 1986; Swirhun *et al*., 1986):

$$\mu_n = 232 + \frac{1180}{1 + \left(\frac{N_A}{8 \times 10^{16}} \right)^{0,9}} \quad \text{(A.18)}$$

$$\tau_n = \frac{1}{3,45 \times 10^{-12} N_A + 0,95 \times 10^{-31} {N_A}^2} \quad \text{(A.19)}$$

μ_p and τ_p are respectively the holes mobility and lifetime defined as (Del Alamo *et al*., 1985):

$$\mu_p = 130 + \frac{370}{1 + \left(\frac{N_D}{8 \times 10^{17}} \right)^{1,25}} \quad \text{(A.20)}$$

$$\tau_p = \frac{1}{7,8 \times 10^{-13} N_D + 1,7 \times 10^{-31} {N_D}^2} \quad \text{(A.21)}$$

The carrier densities and the currents in base and emitter region were calculated for k and j varying from 1 to 10, which has been found to be sufficient to obtain a good convergence whatever the grain dimensions and the superficial recombination velocities.

Dark current

In order to calculate the dark current in the base region, one solves the continuity equation which is given by:

$$\frac{\partial^2 \Delta n}{\partial z^2} + \frac{\partial^2 \Delta n}{\partial x^2} - \frac{\Delta n}{{L_n}^2} = 0 \quad \text{(A.22)}$$

With the general solution:

$$\Delta n(x,z) = \sum_{k=1}^{\infty} g_k(z) \cos\left(J_k \left(x - d/2 \right) \right) \quad \text{(A.23)}$$

Using the same method in section A.1, g_k is expressed under the shape:

$$g_k(z) = \frac{4 {n_i}^2 \sin\left(J_k \frac{d}{2} \right)}{N_A \left(J_k d + \sin\left(J_k d \right) \right)} \left[\frac{sh\left(\frac{H - z}{L_k} \right) + \frac{D_n}{L_k S_n} ch\left(\frac{H - z}{L_k} \right)}{sh\left(\frac{W_b}{L_k} \right) + \frac{D_n}{L_k S_n} ch\left(\frac{W_b}{L_k} \right)} \right]$$

The saturation diffusion dark current I_{d0} is given by:

$$I_{d0} = I_{b0} + I_{e0}$$

Where I_{b0} and I_{e0} are respectively the dark current in base and emitter region obtained by the same formula in (A.6) and (A.7) given respectively by:

$$I_{b0} = S' \sum_{k=1}^{\infty} \frac{-8qn_i^2 \sin\left(J_k \frac{d}{2}\right)^2 D_n}{J_k L_k dN_A \left(J_k d + \sin\left(J_k d\right)\right)} \times \left\{ \frac{ch\left(\frac{W_b}{L_k}\right) + \frac{D_n}{L_k S_n} sh\left(\frac{W_b}{L_k}\right)}{sh\left(\frac{W_b}{L_k}\right) + \frac{D_n}{L_k S_n} ch\left(\frac{W_b}{L_k}\right)} \right\} \quad \text{(A.24)}$$

$$I_{e0} = S' \sum_{j=1}^{\infty} \frac{8qn_i^2 \sin\left(J_j \frac{D}{2}\right)^2 D_p}{J_j L_j DN_D \left(J_j D + \sin\left(J_j D\right)\right)} \times \left\{ \frac{ch\left(\frac{W_e}{F_j}\right) + \frac{D_p}{F_j S_p} sh\left(\frac{W_e}{F_j}\right)}{sh\left(\frac{W_e}{F_j}\right) + \frac{D_p}{F_j S_p} ch\left(\frac{W_e}{F_j}\right)} \right\} \quad \text{(A.25)}$$

The J_k and J_j coefficients are obtained by the following transcendental equation:

$$tg\left(J_k \frac{d}{2}\right) = \frac{V_g}{2J_k D_n} \quad \text{(A.26)}$$

$$tg\left(J_j \frac{D}{2}\right) = \frac{V}{2D_p J_j} \quad \text{(A.27)}$$

The saturation recombination current I_{r0} is given by (Sze, 1991):

$$I_{r0} = \frac{S' qWn_i}{\sqrt{\tau_n \tau_p}} \quad \text{(A.28)}$$

REFERENCES

Ba, B. and Kane, M. 1995. Open-circuit voltage decay in polycristalline silicon solar cells. *Sol. Energ. Mat. and Sol. Cells*, 37: 259-271.

Ben Arab, A. 1997. Modelling of the recombination at grain boundaries in preferentially doped polysilicon solar cells. *Solid-State Electron*., 41(9): 1355-1362.

Ben Amar, M., Ben Arab, A. 2001. Comparison between grain boundary theories in polycrystalline silicon. *Rev. Int. d'Héliotechnique*, 3: 24-27.

Ben Amar, M. and Ben Arab, A. 2003. Improved modelling of grain boundary recombination in polycrystalline silicon under excitation. *Phys. Chem. News*, 9: 67-74.

Belghachi, A. and Helmaoui, A. 2008. Effect of the front surface field on GaAs solar cell photocurrent. *Sol. Energ. Mat. & Sol. Cells*, 92: 667-672.

Del Alamo, J., Swirhun, S. and Swanson, R. 1985. Simultaneous measurement of hole lifetime, hole mobility and bandgap-narrowing in heavily doped n-type silicon. *IEDM techn. Dij*., p. 290-293.

Diallo, H.L., Seïdou Maiga, A., Wereme, A. and Sissoko, G. 2008. New approach of both junction and back surface recombination velocities in a 3D modelling study of a polycrystalline silicon solar cell. *The Euro. Phys. J. App. Phys*., 42: 203-211.

Dugas, J. 1994. 3D modelling of a reverse cell made with improved multicrystalline silicon wafers. *Sol. Energ. Mat. & Sol. Cells*, 32: 71-88.

Dugas, J. 1996. Modelling of material properties influence on back junction thin polycristalline silicon solar cells. *Sol. Energ. Mat. & Sol. Cells*, 43: 193-202.

Dugas, J., Crest, J.P., Signal, C.M. and Oualid, J. 1983. Grain boundary barrier height in base and space charge regions. *Solid-State Electron*., 26(11): 1069-1075.

Dugas, J. and Oualid, J. 1987. 3D-modelling of polycrystalline silicon solar cells. *Rev. Phys. Appl.*, 22: 677-685.

Green, M.A. 1978. Photocurrent loss within the depletion region of polycrystalline solar cells. *Solid-State Electron*., 21: 1139-1144.

Halder, N.C., Williams, T.R. 1983. Grain boundary effects in polycrystalline silicon solar cells. I- Solution of the three-dimensional diffusion equation by the Green's function method. II- Numerical calculation of the limiting parameters and maximum efficiency. *Sol. Cells*, 8: 201-223, 225-238.

Hovel, H.J. 1975. Semiconductors and semimetals. In: R.K Willardson and A.C. Beer (eds), *Sol. Cells*, 11: 15-24, New York, Academic Press.

Joshi P, D. and Bhatt, D. P. 1990. Theory of grain boundary recombination and carrier transport in polycrystalline silicon under optical illumination. *IEEE Trans. On Electron. Dev.*, 37(1): 237.

King, D.L., Dudley, J.K. and Boyson, W.E. 1996. PVSIM: a simulation program for photovoltaic cells, modules and arrays. *In:* the 25th IEEE Photovoltaic Specialists Conference, pp. 1295-1297.

Kotsovos, K. and Perraki, V. 2005. Structure optimization according to a 3D model applied on epitaxial Si solar cells: A comparative study. *Sol. Energ. Mat. & Sol. Cells*, 89: 113-127.

Liou, J.J. and Wong, W.W. 1992. Comparison and optimization of the performance of Si and GaAs solar cells. *Sol. Energ. Mat. & Sol. Cells*, 28: 9-28.

Masetti, G. Severi, M. and Solmi, S. 1983. Modelling of carrier mobility against carrier concentration in arsenic-, phosphorus-, and boron-doped silicon. *IEEE Trans. On Electron. Dev.*, 30(7): 764-769.

Mohammed, S.N., Sobhan M.A. and Qutubuddin S. 1989. The influence of grain boundaries on the performance efficiency of polycrystalline gallium arsenide solar cells. *Solid-State Electron*., 32 (10): 827-834.

Mohammed, S.N., Rogers C.E. 1988. Current-voltage characteristics and performance efficiency of Polysilicon solar cells. *Solid-State Electron*., 31 (8): 1221-1228.

Oualid, J., Signal, C.M., Dugas, J., Grest, J.P. and Amzil, H. 1984. Influence of the illumination on the grain boundary recombination velocity in silicon. *J. App. Phys.*, 55(4): 1195-1205.

Swirhun, S., Kwark , Y.H. and Swanson, R.M. 1986. Measurement of electron lifetime, electron mobility and bandgap narrowing in heavily doped p-type silicon. *IEDM Techn. Dij*., pp. 24-27.

Sze, S.M. 1991. In: *Physics of semiconductor devices*. New Jersey, Murry Hill: Bell laboratories Inc.

Van Dyk, E.E. and Meyer, E.L. 2004. Analysis of the effect of parasitic resistances on the performance of photovoltaic modules. *Renew. Energ*., 29: 333-344.

Zhao, L., Li, H.L., Zhou, C.L., Diao, H.W. and Wang, W.J. 2009. Optimized resistivity of p-type Si substrate for HIT solar cell with Al back surface field by computer simulation. *Sol. Energ*., 83: 812-816.